

PAPER

## Directed momentum current of Bose–Einstein condensate in the presence of spatially modulated nonlinear interaction

To cite this article: Wen-Lei Zhao *et al* 2016 *J. Phys. B: At. Mol. Opt. Phys.* **49** 125303

View the [article online](#) for updates and enhancements.

### You may also like

- [Millimeter Light Curves of Sagittarius A\\* Observed during the 2017 Event Horizon Telescope Campaign](#)  
Maciek Wielgus, Nicola Marchili, Iván Martí-Vidal *et al.*
- [A Universal Power-law Prescription for Variability from Synthetic Images of Black Hole Accretion Flows](#)  
Boris Georgiev, Dominic W. Pesce, Avery E. Broderick *et al.*
- [Broadband Multi-wavelength Properties of M87 during the 2017 Event Horizon Telescope Campaign](#)  
The EHT MWL Science Working Group, J. C. Algaba, J. Anzarski *et al.*



**IOP | ebooks™**

Bringing together innovative digital publishing with leading authors from the global scientific community.

Start exploring the collection—download the first chapter of every title for free.

# Directed momentum current of Bose–Einstein condensate in the presence of spatially modulated nonlinear interaction

Wen-Lei Zhao<sup>1,2,3</sup>, Cai-Ying Ding<sup>1</sup>, Jie Liu<sup>2,3</sup> and Li-Bin Fu<sup>2,3</sup>

<sup>1</sup>School of Science, Jiangxi University of Science and Technology, Ganzhou 341000, People's Republic of China

<sup>2</sup>National Laboratory of Science and Technology on Computational Physics, Institute of Applied Physics and Computational Mathematics, Beijing 100088, People's Republic of China

<sup>3</sup>HEDPS, Center for Applied Physics and Technology, Peking University, Beijing 100084, People's Republic of China and CICIFSA MoE College of Engineering, Peking University, Beijing 100871, People's Republic of China

E-mail: [liu\\_jie@iapcm.ac.cn](mailto:liu_jie@iapcm.ac.cn) and [lbfu@iapcm.ac.cn](mailto:lbfu@iapcm.ac.cn)

Received 27 September 2015, revised 1 April 2016

Accepted for publication 26 April 2016

Published 18 May 2016



CrossMark

## Abstract

We investigate the quantum transport dynamics of periodically delta-kicked Bose–Einstein condensate under the effect of spatially modulated nonlinear interactions. The spatial modulation frequency can dramatically affect the transport behaviors of the ultra-cold atoms. For odd frequency, the linear growth of the directed current is close to that of the noninteracting case for not very strong nonlinear interaction. Both the acceleration and the quantum state evolution gradually approach that of the noninteracting case with increasing frequency. For other values of frequency, a very weak nonlinear interaction can dramatically reduce the linear growth of the directed current. The quantum state evolution differs rapidly from that of the noninteracting case. The underlying dynamic mechanism is uncovered and some important implications are addressed.

Keywords: Bose–Einstein condensate, directed transport, coherent manipulation

(Some figures may appear in colour only in the online journal)

## 1. Introduction

Directed transport, which is usually referred to as ratchets phenomenon [1–3], has recently gained renewed interest as its mechanism is relevant for the construction of nanoscale devices, such as particle separation and electron pumps, and for the understanding of biological molecular motors [4–7]. The breaking of spatial-temporal symmetry ensures the occurrence of directed transport. Bose–Einstein condensate (BEC) atoms which are loaded in an optical lattice are an ideal system for investigating ratchets phenomenon [8]. On the condition that the optical lattice is spatially asymmetric [9, 10] or that its phase is asymmetrically modulated in time [11], BEC atoms exhibit directed motion. A number of BEC experiments have observed the directed momentum current which is caused by the delta-kicking optical lattice under quantum resonance conditions [12–16].

The realization of dilute BEC gases has opened new opportunities for studying dynamical systems in the presence of many-body interactions. The mean-field treatment of the interactions between atoms induces a nonlinear modification to the Schrödinger equation. Interestingly, the nonlinear interaction can give rise to directed transport [17, 25], and can destroy the ballistic diffusion [18] of delta-kicked BEC atoms in the quantum resonance case. A recent trend in atom optics concerns the quantum dynamics of BEC atoms under the effect of spatially modulated nonlinear interactions [19]. Indeed, significant progress in the atom optics technique allows spatial modulation of the atomic interaction strength via optical standing wave [20, 21] or magnetic field [22]-induced Feshbach resonance management. In such contexts, understanding the ratchet effects in the presence of spatially modulated nonlinear interaction is of great importance.

In this paper, we numerically investigate the directed momentum current of delta-kicked BEC atoms under the effects of spatially modulated nonlinear interactions of the form  $g_0 \sin(\gamma\theta)|\psi|^2$ , where  $g_0$  is nonlinear strength and  $\gamma$  denotes spatial modulation frequency. Without nonlinear interaction, i.e.,  $g_0 = 0$  or  $\gamma = 0$ , the periodic kick in the quantum resonance condition leads to linear growth of the momentum current with time [23, 24]. In this work, we numerically investigate the generation of the momentum current under the effects of nonlinear interaction, which can be controlled by adjusting the parameters  $g_0$  and  $\gamma$ .

Our numerical results show that, for fixed  $\gamma$ , the acceleration of the directed momentum current gradually decreases to zero with increasing  $g_0$ , which demonstrates the suppression of the directed transport of BEC atoms by nonlinear interaction. Such a phenomenon is similar to that of a delta-kicked BEC system whose nonlinear interaction is unmodulated (i.e.,  $g_0|\psi|^2$ ) [25]. We further numerically investigate the nonlinear effects on momentum current for a wide range of  $\gamma$ . Interestingly, for odd values of  $\gamma$ , the suppression of the directed motion by nonlinearity is apparent only for a large enough  $g_0$ . In this situation, the acceleration of the momentum current approaches that of the noninteracting case ( $g_0 = 0$  or  $\gamma = 0$ ) with increasing  $\gamma$ , which demonstrates the disappearance of the nonlinearity effects. Thus, the spatial modulation seems to reduce nonlinearity effects. For other values of  $\gamma$ , a very weak nonlinear strength is able to dramatically reduce the generation of the momentum current. In this situation, nonlinearity effects are reinforced by spatial modulation.

The dependence of nonlinear effects on the spatial modulation is confirmed by the fidelity of quantum states between the interacting and noninteracting case. Our numerical results show that, for odd values of  $\gamma$  with a fixed  $g_0$ , the fidelity decays from unity to saturation levels as time evolves. Moreover, the saturation level increases with increasing  $\gamma$ . For other values of  $\gamma$ , the fidelity rapidly decays from unity to almost zero as time evolves. Therefore, the time-averaged fidelity is almost zero except for some peaks corresponding to odd values of  $\gamma$ . In addition, the values of peaks gradually approach unity with increasing  $\gamma$ . In order to reveal the underlying mechanism, we analytically study the time evolution of the quantum states in the presence of the nonlinear interaction. Our approximated analysis shows that, for odd values of  $\gamma$ , the nonlinearity effects at different times cancel each other; thus the quantum state revives after the evolution over a period of  $T = 4\pi$ . Such periodic revival is a character of quantum resonance in the noninteracting case. For even values of  $\gamma$ , the nonlinear effects at different times are mutually enforced. As a consequence, the wave packets gradually differ from that of the noninteracting case with time evolution. In this situation, we analytically obtained an approximated expression of the quantum state at time  $T = 4\pi$ . We use this state to numerically calculate the growth rate of the momentum current for a wide region of  $g_0$ . It qualitatively shows the reduction, reversal, and finally the disappearance of the directed momentum current with the increase in strength of the nonlinear interaction.

The paper is organized as follows. In section 2, we describe the system and show the momentum current in the presence of spatially modulated nonlinear interaction. In section 3, we study the wave packet dynamics, including the probability density distribution in momentum space and the fidelity of the quantum state between the interacting and noninteracting case. An analytical study of the time evolution of the quantum state is presented in section 4. Section 5 concludes this work.

## 2. Directed momentum current

We consider the following BEC model with a spatially modulated interaction. Taking the Planck constant  $\hbar$ , the single-particle mass and the radius of the ring, the BEC satisfies the following dimensionless Gross–Pitaevskii equation (GPE),

$$i\frac{\partial}{\partial t}\psi = \left[ \frac{p^2}{2} + K \cos(\theta)\delta_T + g_0 \sin(\gamma\theta)|\psi|^2 \right] \psi, \quad (1)$$

where  $p = -i\partial/\partial\theta$ ,  $K$  is the kick strength, and  $\delta_T = \sum_j \delta(t - jT)$  with  $T$  the kick period. Due to the significant progress achieved in the past years in the techniques of managing the atomic scattering strength by means of Feshbach resonance [26], the nonlinear interaction strength in the GPE can be spatially modulated [20–22].

When  $g_0 = 0$ , the system has spatial and time-reversal symmetries, in which the emergence of the directed transport requires the rectification of kicking force that can be realized by setting an asymmetric initial wave packet. Experimentally using the Bragg pulse, one can prepare a superposition state of the form  $|\psi\rangle_{\text{ini}} = \frac{1}{\sqrt{2}}[|0\rangle + e^{i\phi}|-1\rangle]$  with a relative phase factor  $\phi$  [13]. For  $g_0 = 0$ , the quantum state can revive exactly at a period duration of the Talbot time ( $T = 4\pi$ ) [27, 28]. In this situation, the average momentum takes the form  $\langle p(t) \rangle = \langle p_0 \rangle + \frac{K}{2} \sin(\phi)t$ , where  $\langle p_0 \rangle$  is the initial value. Such linear growth of the average momentum with time indicates the emergence of directed current in momentum space. The acceleration (or growth rate) is  $R = d\langle p \rangle/dt = K \sin(\phi)/2$ .

In order to investigate the momentum current of the nonlinear system, we solve the nonlinear Schrödinger equation numerically using the splitting operator method [29]. Figure 1(a) shows the time dependence of  $\langle p \rangle$  for  $\gamma = 2$  with various  $g_0$ . We see that for weak nonlinearity (e.g.,  $g_0 = 0.1$  and  $0.2$ ), the linear growth rate of the momentum current is much smaller than that of the noninteracting case ( $g_0 = 0$ ). With an increase in the nonlinearity to  $g_0 = 1$ , the momentum current reverses direction and its growth rate changes to negative. Such consecutive acceleration of the momentum current to the negative direction is different from the current reversal in [12, 30] where the growth in momentum current saturates as time evolves. At strong nonlinearity of  $g_0 = 3$ , the momentum current almost vanishes. The above observations are more clearly demonstrated in figure 1(b), in which the acceleration  $R$  for  $\gamma = 2$  decreases from  $0.37 \left( = \frac{K}{2} \right)$  to a

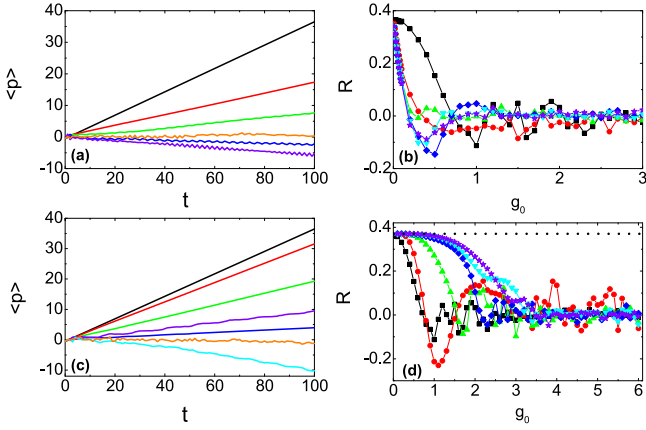


**Figure 1.** Left panels: time dependence of the average momentum  $\langle p \rangle$  for  $\gamma = 2$  (top) and 3 (bottom), respectively. (a) From top to bottom  $g_0 = 0$  (black line), 0.1 (red line), 0.2 (green line), 3 (orange line), 0.4 (blue line) and 1 (violet line). (c) From top to bottom  $g_0 = 0$  (black line), 0.8 (red line), 1.2 (green line), 2 (violet line), 1.5 (blue line), 4 (orange line) and 3 (cyan line). Time is measured in the number of kick periods ( $T = 4\pi$ ). Right panels: the acceleration  $R$  versus  $g_0$  for even (top) and odd (bottom)  $\gamma$ , respectively. (b)  $\gamma = 2$  (red circles), 4 (green up triangles), 6 (blue diamonds), 8 (cyan down triangles) and 10 (violet pentagrams). (d)  $\gamma = 1$  (red circles), 3 (green up triangles), 5 (blue diamonds), 7 (cyan down triangles) and 9 (violet pentagrams). In (b) and (d), for comparison, the values of  $R$  of unmodulated nonlinear interaction (i.e.,  $g_0|\psi|^2$ ) are denoted by the black squares. In (d), the dotted line denotes  $R = 0.37$  which is the acceleration of the noninteracting case (i.e.,  $g_0 = 0$ ). The parameters are:  $K = 0.74$ ,  $T = 4\pi$  and  $\phi = \frac{\pi}{2}$ .

negative value  $-0.05$ , oscillates, and finally converges into zero after  $g = 1.5$ . Moreover, for  $\gamma = 2$ , the decrease of  $R$  with  $g_0$  is much faster than that of the unmodulated nonlinearity. This demonstrates that the spatially modulated nonlinearity can dramatically suppress the generation of the momentum current. Such suppression of momentum current by the nonlinearity is a common phenomenon for even values of  $\gamma$  (see figure 1(b)).

For odd values of  $\gamma$ , the nonlinearity effects on the momentum current become weak. Figure 1(c), for  $\gamma = 3$ , shows that the momentum current has a small difference from that of the noninteracting case even when  $g_0 = 0.8$ , for which the directed current almost disappears with  $\gamma = 2$  (see figure 1(b)). With increasing  $g_0$ , the momentum current reduces and reverses direction (e.g., for  $g_0 = 3$ ). For much stronger  $g_0$  (e.g.,  $g_0 = 4$ ), the value of  $\langle p \rangle$  is almost zero with time evolution, which demonstrates the disappearance of the momentum current. We also numerically investigate the dependence of the acceleration  $R$  on  $g_0$ , which is shown in figure 1(d). We can see that, for a specific  $\gamma$ , the value of  $R$  decreases from 0.37 to almost zero with increasing  $g_0$ , which demonstrates the suppression of the momentum current by nonlinear interaction. Detailed investigations show that the acceleration approaches that of the noninteracting case with increasing  $\gamma$ . This clearly demonstrates that nonlinearity effects become weak with the increase in  $\gamma$ .

From the above results, we see that the modulation frequency  $\gamma$  is able to control the nonlinearity effects on the

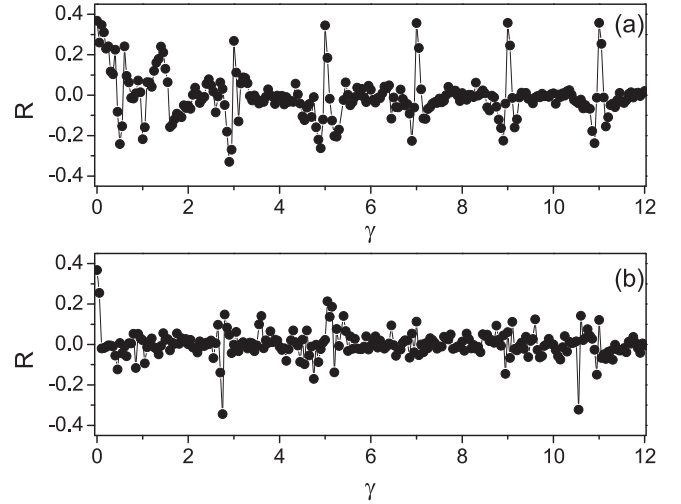


**Figure 2.** The acceleration  $R$  versus  $\gamma$  for  $g_0 = 1$  (top) and 3 (bottom). Other parameters are the same as in figure 1.

directed motion of the BEC atoms. This is more clearly demonstrated in figure 2, which shows the dependence of  $R$  on  $\gamma$  for different  $g_0$ . Figure 2(a), for  $g_0 = 1$ , shows that the acceleration  $R$  rapidly decays from 0.37 to almost zero with increasing  $\gamma$ . Interestingly, it has some peaks corresponding to odd values of  $\gamma$ , except for  $g_0 = 1$ , with which the acceleration is negative. More important is that the acceleration of the peaks gradually approaches 0.37 with increasing  $\gamma$ , which demonstrates the disappearance of nonlinearity effects. However, such dependence of acceleration on  $\gamma$  disappears for strong nonlinearity. Figure 2(b) for  $g_0 = 3$  shows that the acceleration is almost zero for all  $\gamma$ . Since both the spatial modulation of nonlinear interactions [20–22, 26] and the periodically kicked BEC [32–34] are realizable in today’s ultra-cold atom experiments, our investigations may be experimentally observed, and may be helpful for the manipulation of the directed transport of BEC atoms.

### 3. Probability distribution in momentum space

To gain insight into the mechanism of the momentum current of the nonlinear system, we trace the time evolution of the wave packet in momentum space. Figure 3 shows the numerical results for  $\gamma = 3$  with different  $g_0$ . From figure 3(a) we can see that, for  $g_0 = 0$ , the wave packet spreads along the positive momentum direction, which corresponds to the linear growth of the directed current. When the nonlinearity is present (e.g.,  $g = 1.2$  in figure 3(b)), the wave packet in momentum space separates into three portions. One part at  $p = 0$  does not move, and the other two parts move in opposite directions as time evolves. The movement of BEC atoms to negative momentum results in a decrease in the momentum current with respect to the noninteracting case. At higher nonlinearity of  $g = 3.0$  (see figure 3(c)), the portion of BEC atoms moving to a negative direction becomes large, and as a consequence the current changes direction. For adequately strong nonlinearity, our extensive investigations

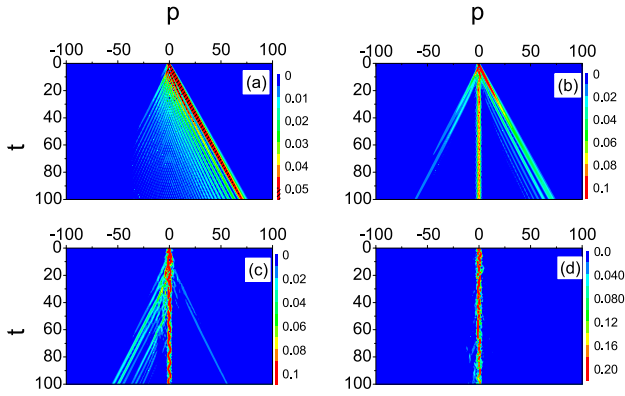


**Figure 3.** Time evolution of the probability density distribution in the momentum space for  $\gamma = 3$  with  $g_0 = 0$  (a), 1.2 (b), 3.0 (c) and 4.0 (d). Other parameters are the same as in figure 1.

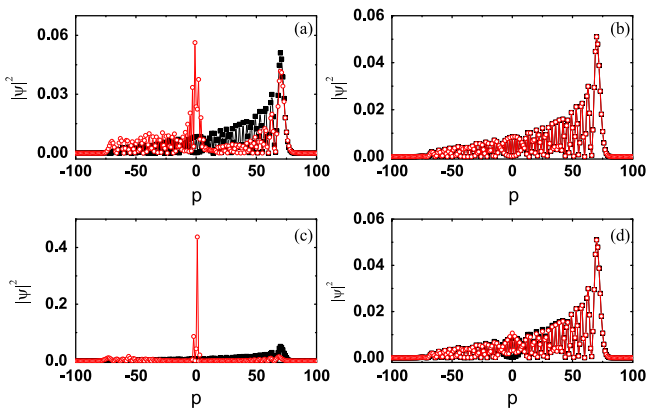
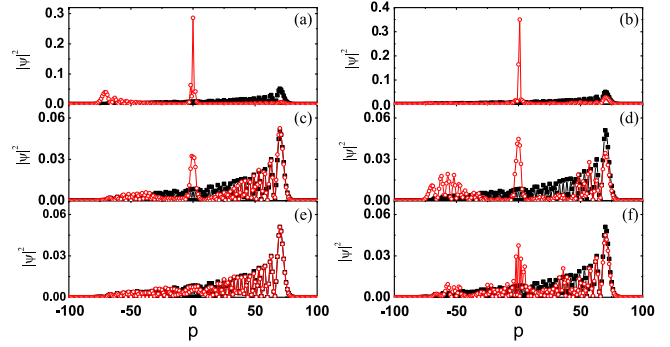


**Figure 4.** The momentum distribution (empty red circles) at  $t = 100$  for  $\gamma = 2$  (left panels) and 3 (right panels) with  $g_0 = 0.1$  (top panels) and 0.4 (bottom panels). The corresponding momentum distributions of the noninteracting case are depicted by solid black squares. Other parameters are the same as in figure 1.

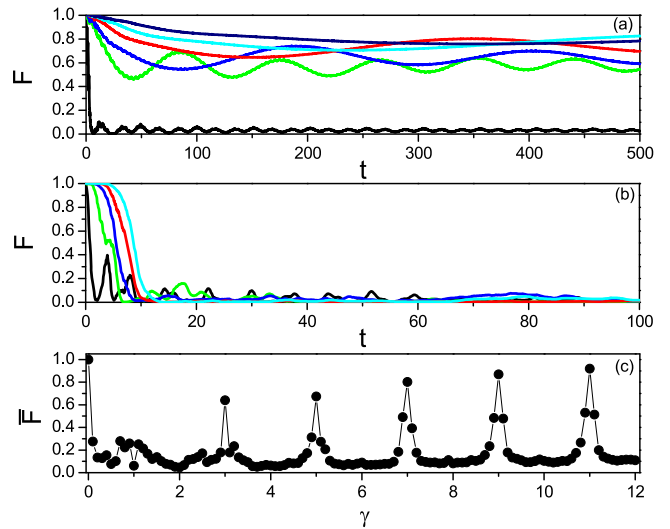
show that the wave packet is localized at the momentum  $p = 0$  (e.g.,  $g_0 = 4$  in figure 3(d)). In this case, the directed momentum current vanishes.

Figure 4 shows the comparison of momentum distributions between the interacting and noninteracting case for different  $g_0$  and  $\gamma$ . We see that, for  $\gamma = 2$ , the momentum distribution of  $g_0 = 0.1$  has an obvious difference from that of the noninteracting case in two aspects: (i) a significant peak around  $p = 0$ ; and (ii) a large fraction of the momentum distribution spreading to the negative momentum (see figure 4(a)). Such difference becomes more evident for large  $g_0$ , e.g.,  $g_0 = 0.4$  (in figure 4(c)) for which momentum distribution has a prominent peak around  $p = 0$ . This demonstrates the dramatic influence of nonlinear interaction on the time evolution of the quantum state. However, for  $\gamma = 3$  (in figure 4(b) and figure 4(d)), the momentum distributions with  $g_0 = 0.1$  and 0.4 are all in good agreement with that of  $g_0 = 0$ , which demonstrates that the spatial modulation of odd  $\gamma$  can reduce nonlinear effects.

In the above section, we show that the current behavior becomes closer to that of the noninteracting case with



**Figure 5.** The momentum distributions (empty red circles) at  $t = 100$  for  $g_0 = 1$  (left panels) and 2 (right panels); from top to bottom  $\gamma = 1, 5$  and 11, respectively. The corresponding momentum distributions of the noninteracting case are depicted by solid black squares. Other parameters are the same as in figure 1.



**Figure 6.** (a) Time dependence of fidelity  $F$  of quantum states between  $g_0 = 1$  and  $g_0 = 0$ , with  $\gamma = 1$  (black line), 3 (green line), 5 (blue line), 7 (red line), 9 (cyan line) and 11 (navy line). (b) Same as in (a) but for  $\gamma = 2$  (black line), 4 (green line), 6 (blue line), 8 (red line) and 10 (cyan line). (c) Time-averaged fidelity  $\bar{F}$  versus  $\gamma$  for  $g_0 = 1$ . Other parameters are the same as in figure 1.

increasing odd  $\gamma$ . This is confirmed by the corresponding momentum distributions. Figure 5(a) shows that, for  $\gamma = 1$ , the momentum distributions between  $g_0 = 1$  and  $g_0 = 0$  have significant differences. Interestingly, such differences gradually disappear with increasing  $\gamma$ , as shown in figure 5(c) with  $\gamma = 5$ . For strong enough nonlinearity, e.g.,  $d = 11$  in figure 5(e), the momentum distributions between  $g_0 = 1$  and  $g_0 = 0$  are in good agreement. The same process occurs for  $g_0 = 2$  with increasing  $\gamma$ , as shown in figure 5(b), figure 5(d) and figure 5(f).

A commonly used measure of the discrepancy between two quantum states is fidelity  $F(t) = |\langle \psi(t) | \varphi(t) \rangle|^2$  [35, 36]. We numerically calculate the fidelity for quantum states between the interacting and noninteracting case. Figure 6(a), for odd values of  $\gamma$ , shows that, with time evolution, the fidelity decays from unity to saturation levels which are much larger than zero except for  $\gamma = 1$ . Interestingly, the saturation

values increase with increasing  $\gamma$ , which proves that the quantum states approach that of the noninteracting case. For even values of  $\gamma$ , the fidelity decays from unity to almost zero (see figure 6(b)), which demonstrates that the quantum states are different from that of the noninteracting case. The above observations are more clearly demonstrated in figure 6(c). We can see that the time-averaged fidelity rapidly decays from unity to almost zero with increasing  $\gamma$ , except for some peaks corresponding to odd  $\gamma$  ( $\gamma > 1$ ). More important is that the time-averaged fidelity of the peaks gradually approaches unity with increasing  $\gamma$ , which reveals the disappearance of nonlinear effects.

#### 4. Effects of spatially modulated nonlinearity on the time evolution of the quantum state

A pictorial explanation is that, for initial probability distribution of the form  $|\psi_{\text{ini}}(\theta)|^2 = [1 + \cos(\theta - \phi)]/(2\pi)$  with  $\phi = \pi/2$ , any perturbation will be maximal if it has a maximal impact at this precise phase angle with respect to the kick potential. For odd  $\gamma$ , the nonlinearity is maximal at this value in  $\theta$  space but its force is zero. For other values of  $\gamma$ , the contrary is true and the effect of the nonlinearity is maximized [30, 31]. In order to reveal how the nonlinear interaction affects the wave packet evolution, we analytically derive the time evolution of the quantum state over a period  $T$ . It is obtained by approximately separating the time evolution of a period into two steps. For the evolution of the state in each time interval ( $\Delta t = T/2$ ), we use the splitting operator method only one time. The evolution operator in the first time interval takes the form

$$U\left(\frac{T}{2}, 0\right) = U_f\left(\frac{T}{2}, \frac{T}{4}\right)U_g\left(\frac{T}{4}\right)U_f\left(\frac{T}{4}, 0\right),$$

where  $U_f(t_2, t_1)$  denotes the free evolution operator, i.e.,

$$U_f(t_2, t_1) = \exp\left(-i\frac{p^2}{2}\frac{t_2 - t_1}{2}\right),$$

and  $U_g\left(\frac{T}{4}\right)$  is the evolution operator of the nonlinear interaction, i.e.,

$$U_g\left(\frac{T}{4}\right) = \exp\left[-ig_0 \sin(\gamma\theta) \left| \psi\left(\theta, \frac{T}{4}\right) \right|^2 \frac{T}{2}\right] \quad (2)$$

with  $\psi\left(\theta, \frac{T}{4}\right) = U_f\left(\frac{T}{4}, 0\right)\psi(\theta, 0)$  being the state after the free evolution of the time interval  $\Delta t = T/4$ . The initial state is  $\psi(\theta, 0) = \{1 + \exp[i(\phi - \theta)]\}/\sqrt{4\pi}$ .

The quantum state at the time  $t = T^-$  takes the form

$$\begin{aligned} \psi(\theta, T^-) &= U\left(T^-, \frac{T}{2}\right)U\left(\frac{T}{2}, 0\right)\psi(\theta, 0) \\ &= U_f\left(T^-, \frac{3T}{4}\right)U_g\left(\frac{3T}{4}\right)U_f\left(\frac{3T}{4}, \frac{T}{4}\right) \\ &\quad \times U_g\left(\frac{T}{4}\right)U_f\left(\frac{T}{4}, 0\right)\psi(\theta, 0), \end{aligned} \quad (3)$$

where the superscript ‘-’ denotes the time immediately before the first kick.

For  $T = 4\pi$ , the free evolution of a quantum state during a time interval of  $T/4$  belongs to the quantum resonance case, i.e.,  $\tau = 4\pi p/q$  with  $p = 1$  and  $q = 4$ . Fortunately, we can obtain an analytical expression for the quantum state  $\psi\left(\theta, \frac{T}{4}\right)$ . The reason is that, for  $\tau = 4\pi p/q$ , the analytical expression of the quantum state  $\psi(\theta, \tau)$  [17, 28] can be expressed as

$$\psi(\theta, \tau) = \sum_{n=0}^{q-1} C_n \psi\left(\theta + 2\pi\frac{n}{q}, 0\right), \quad (4)$$

with the coefficients

$$C_n = \frac{1}{q} \sum_{m=0}^{q-1} \exp\left(-i\frac{2\pi p}{q}m^2 - i\frac{2\pi mn}{q}\right). \quad (5)$$

According to equations (4) and (5), we get

$$\psi\left(\theta, \frac{T}{4}\right) = \frac{1}{\sqrt{2}}e^{-i\pi/4}\psi(\theta, 0) + \frac{1}{\sqrt{2}}e^{i\pi/4}\psi(\theta + \pi, 0). \quad (6)$$

For  $\psi(\theta, 0) = \{1 + \exp[i(\phi - \theta)]\}/\sqrt{4\pi}$ ,

$$\left| \psi\left(\theta, \frac{T}{4}\right) \right|^2 = \frac{1}{\sqrt{2\pi}}[1 + \sin(\phi - \theta)].$$

Then, according to equation (2), the nonlinear evolution operator at the time  $t = T/4$  takes the form

$$U_g\left(\frac{T}{4}\right) = \exp\{-ig_0 \sin(\gamma\theta)[1 + \sin(\phi - \theta)]\}.$$

After the acting of  $U_g$  on  $\psi\left(\theta, \frac{T}{4}\right)$ , the quantum state is

$$\begin{aligned} \psi_g\left(\theta, \frac{T}{4}\right) &= \exp\{-ig_0 \sin(\gamma\theta)[1 + \sin(\phi - \theta)]\} \\ &\quad \times \psi\left(\theta, \frac{T}{4}\right). \end{aligned}$$

The next step is the free evolution of the quantum state  $\psi_g\left(\theta, \frac{T}{4}\right)$  from the time  $t = T/4$  to  $3T/4$  (see equation (3)). In this situation, the time interval equals  $\tau = 2\pi$ . Then, according to equations (4) and (5), we can obtain

$$\begin{aligned} \psi\left(\theta, \frac{3T}{4}\right) &= \psi_g\left(\theta + \pi, \frac{T}{4}\right) \\ &= \exp\{-ig_0 \sin(\gamma\theta + \gamma\pi)[1 - \sin(\phi - \theta)]\} \\ &\quad \times \psi\left(\theta + \pi, \frac{T}{4}\right). \end{aligned} \quad (7)$$

The modular square of the above state takes the form

$$\left| \psi\left(\theta, \frac{3T}{4}\right) \right|^2 = \frac{1}{2\pi}[1 - \sin(\phi - \theta)].$$

Then, the nonlinear evolution operator at the time  $t = 3T/4$  is

$$U_g\left(\frac{3T}{4}\right) = \exp\left[-ig_0 \sin(\gamma\theta) \left|\psi\left(\theta, \frac{3T}{4}\right)\right|^2 \frac{T}{2}\right] \\ = \exp\{-ig_0 \sin(\gamma\theta)[1 - \sin(\phi - \theta)]\}.$$

After the acting of  $U_g\left(\frac{3T}{4}\right)$  on  $\psi\left(\theta, \frac{3T}{4}\right)$ , the quantum state is expressed as

$$\psi_g\left(\theta, \frac{3T}{4}\right) = \exp\{-ig_0 \sin(\gamma\theta)[1 - \sin(\phi - \theta)]\} \\ \times \psi\left(\theta, \frac{3T}{4}\right).$$

Inserting equation (7) in the above equation yields

$$\psi_g\left(\theta, \frac{3T}{4}\right) = \exp\{-ig_0[1 - \sin(\phi - \theta)] \\ \times [\sin(\gamma\theta) + \sin(\gamma\theta + \gamma\pi)]\} \psi\left(\theta + \pi, \frac{T}{4}\right) \\ = \exp[-i\Phi(\theta, \gamma)] \psi\left(\theta + \pi, \frac{T}{4}\right), \quad (8)$$

where the phase factor is

$$\Phi(\theta, \gamma) = g_0[1 - \sin(\phi - \theta)][\sin(\gamma\theta) + \sin(\gamma\theta + \gamma\pi)].$$

For odd  $\gamma$ ,  $\sin(\gamma\theta) + \sin(\gamma\theta + \gamma\pi) = 0$ , which implies that the nonlinearity effects at different steps cancel each other. As a consequence, the phase factor is zero, i.e.,  $\Phi = 0$ . In this case, the quantum state  $\psi_g\left(\theta, \frac{3T}{4}\right)$  takes the form

$$\psi_g\left(\theta, \frac{3T}{4}\right) = \psi\left(\theta + \pi, \frac{T}{4}\right).$$

Then, according to equations (4) and (5), the free evolution of the wave function  $\psi_g\left(\theta, \frac{3T}{4}\right)$  from the time  $t = 3T/4$  to  $t = T^-$  yields

$$\psi(\theta, T^-) = \frac{1}{\sqrt{2}} e^{-i\pi/4} \psi\left(\theta + \pi, \frac{T}{4}\right) \\ + \frac{1}{\sqrt{2}} e^{i\pi/4} \psi\left(\theta, \frac{T}{4}\right). \quad (9)$$

By inserting equation (6) in equation (9), we obtain

$$\psi(\theta, T^-) = \psi(\theta, 0). \quad (10)$$

The above equation shows that the quantum state revives exactly after the time evolution of  $T = 4\pi$ , which is a characteristic of quantum resonance of the noninteracting case. Our approximated analysis may explain why the nonlinearity effects disappear for odd  $\gamma$ .

For even  $\gamma$ ,  $\sin(\gamma\theta) + \sin(\gamma\theta + \gamma\pi) = 2 \sin(\gamma\theta)$ , which means that the nonlinearity effects at different steps enforce

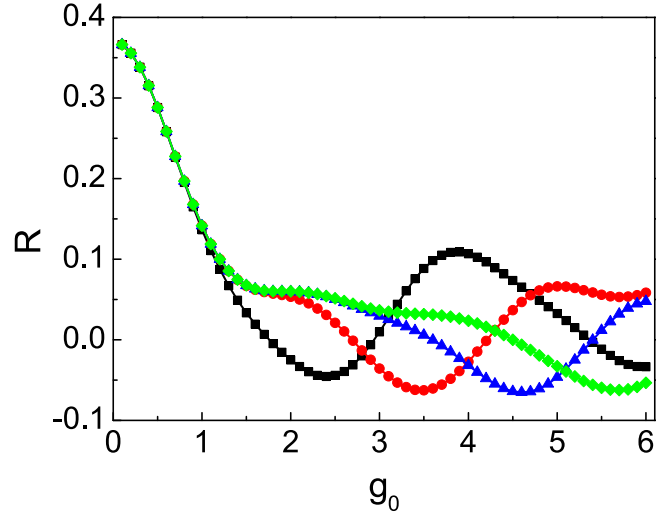


**Figure 7.** The acceleration  $R$  at  $t = 1$  versus  $g_0$  for  $\gamma = 4$  (black squares), 6 (red circles), 8 (blue triangles) and 10 (green diamonds). Other parameters are the same as in figure 1.

each other. The quantum state  $\psi_g\left(\theta, \frac{3T}{4}\right)$  takes the form

$$\psi_g\left(\theta, \frac{3T}{4}\right) = \exp\{-i2g_0 \sin(\gamma\theta)[1 - \sin(\phi - \theta)]\} \\ \times \psi\left(\theta + \pi, \frac{T}{4}\right).$$

According to equations (4) and (5), the free evolution of the wave function  $\psi_g\left(\theta, \frac{3T}{4}\right)$  from time  $t = 3T/4$  to  $t = T^-$  yields

$$\psi(\theta, T^-) = \exp[-i2g_0 \sin(\gamma\theta)] \\ \times \{\psi(\theta, 0) \cos[2g_0 \sin(\gamma\theta) \cos(\theta)] \\ + \psi(\theta + \pi, 0) \sin[2g_0 \sin(\gamma\theta) \cos(\theta)]\}. \quad (11)$$

After the first kick, the quantum state is

$$\psi(\theta, T^+) = \exp[-iK \cos(\theta)] \exp[-i2g_0 \sin(\gamma\theta)] \\ \times \{\psi(\theta, 0) \cos[2g_0 \sin(\gamma\theta) \cos(\theta)] \\ + \psi(\theta + \pi, 0) \sin[2g_0 \sin(\gamma\theta) \cos(\theta)]\}. \quad (12)$$

Since the momentum current almost linearly increases with time, we can roughly regard the acceleration  $R$  at  $t = T$  as that of the long time behaviors. By using the approximated expression of the wave function in equation (12), we numerically calculate the acceleration  $R$  for a wide regime of  $g_0$ , which is shown in figure 7. We see that, for a specific  $d$ , the  $R$  decreases from  $0.37$  ( $=\frac{K}{2}$ ) to almost zero with increasing  $g_0$ , which is qualitatively consistent with the numerical results of  $R$  in figure 1.

## 5. Conclusion

In this work, we have investigated, both numerically and analytically, the quantum resonance ratchets of the

periodically kicked BEC in the presence of spatially modulated nonlinear interaction. Our numerical results show that nonlinearity effects on the directed motion of BEC atoms can be controlled by the spatial modulation frequency. For odd values of  $\gamma$ , the current behavior has an apparent difference from that of the noninteracting case only for strong enough nonlinear interaction. Both the acceleration of the momentum current and the quantum state gradually approach the noninteracting case with increasing  $\gamma$ . Therefore, the spatial modulation seems to suppress the nonlinear interactions. Our approximated analysis shows that the nonlinearity effects at different time steps cancel each other, thus the quantum state revives after one period time evolution, which is a characteristic of the quantum resonance phenomenon.

For other values of  $\gamma$ , the nonlinear interactions can dramatically reduce the generation of the momentum current with respect to the noninteracting case. Moreover, the acceleration of momentum current is much smaller than that of the unmodulated case, which demonstrates that the spatial modulation enhances nonlinearity effects. This is because nonlinear effects at different time steps enhance each other. In this situation, the quantum state rapidly differs from the noninteracting case, which is characterized by the fast decay of the fidelity from unity to almost zero, as time evolves. By using an approximated expression of the quantum state after one period time evolution, we numerically investigate the acceleration of the momentum current, which qualitatively shows the reduction and reversal of directed current by the nonlinearity. We expect that our investigations may be useful for the coherent manipulation of the quantum transport of BEC atoms.

## Acknowledgments

The authors are grateful to Jiao Wang for stimulating discussions. This work is supported by the National Basic Research Program of China (973 Program) (Grant No. 2013CBA01502, No. 2011CB921503 and No. 2013CB834100) and the National Natural Science Foundation of China (Grant No. 11447016, No. 11374040, No. 11274051 and No. 11475027).

## References

- [1] Feynman R P, Leighton R B and Sands M 1966 *The Feynman Lectures on Physics* vol 1 (Addison-Wesley, Reading) ch 46
- [2] Reimann P 2002 *Phys. Rep.* **361** 57
- [3] Hänggi P and Marchesoni F 2009 *Rev. Mod. Phys.* **81** 387
- [4] Kohler S, Lehmann J and Hänggi P 2005 *Phys. Rep.* **406** 379
- [5] Jülicher F, Ajdari A and Prost J 1997 *Rev. Mod. Phys.* **69** 1269
- [6] Astumian R D 1997 *Science* **276** 917  
Astumian R D and Hänggi P 2002 *Phys. Today* **55** 33
- [7] Lehmann J, Kohler S, Hänggi P and Nitzan A 2002 *Phys. Rev. Lett.* **88** 228305
- [8] Gabriel G C, Giuliano B, Giulio C, Sandro W, Oliver M, Riccardo M and Ennio A 2006 *Phys. Rev. A* **74** 033617
- [9] Renzoni F 2005 *Contemp. Phys.* **46** 161
- [10] Salger T, Kling S, Hecking T, Geckeler C, Morales- Molina L and Weitz M 2009 *Science* **326** 1241
- [11] Gong J B and Brumer P 2006 *Phys. Rev. Lett.* **97** 240602  
Wang J and Gong J B 2008 *Phys. Rev. E* **78** 036219
- [12] Sadgrove M and Wimberger S 2009 *New J. Phys.* **11** 083027
- [13] Sadgrove M, Horikoshi M, Sekimura T and Nakagawa K 2007 *Phys. Rev. Lett.* **99** 043002
- [14] Dana I, Ramareddy V, Talukdar I and Summy G S 2008 *Phys. Rev. Lett.* **100** 024103
- [15] Sadgrove M, Schell T, Nakagawa K and Wimberger S 2013 *Phys. Rev. A* **87** 013631
- [16] White D H, Ruddell S K and Hoogerland M D 2013 *Phys. Rev. A* **88** 063603
- [17] Poletti D, Carlo G G and Li B 2007 *Phys. Rev. E* **75** 011102  
Poletti D, Benenti G, Casati G and Li B 2007 *Phys. Rev. A* **76** 023421  
Poletti D, Benenti G, Casati G, Hänggi P and Li B 2009 *Phys. Rev. Lett.* **102** 130604
- [18] Sandro W, Riccardo M, Oliver M and Ennio A 2005 *Phys. Rev. Lett.* **94** 130404
- [19] Kartashov Y V, Malomed B A and Torner L 2011 *Rev. Mod. Phys.* **83** 247
- [20] Fedichev P O, Yu Kagan, Shlyapnikov G V and Walraven J T M 1996 *Phys. Rev. Lett.* **77** 2913  
Theis M, Thalhammer G, Winkler K, Hellwig M, Ruff G, Grimm R and Hecker Denschlag J 2004 *Phys. Rev. Lett.* **93** 123001
- [21] Timmermans E, Tommasini P, Hussein M and Kerman A 1999 *Phys. Rep.* **315** 199
- [22] Inouye S, Andrews M R, Stenger J, Miesner H J, Stamper-Kurn D M and Ketterle W 1998 *Nature* **392** 151
- [23] Lundh E and Wallin M 2005 *Phys. Rev. Lett.* **94** 110603
- [24] Kenfack A, Gong J B and Pattanayak A K 2008 *Phys. Rev. Lett.* **100** 044104  
Ho D Y H and Gong J B 2012 *Phys. Rev. Lett.* **109** 010601
- [25] Zhao W L, Fu L B and Liu J 2014 *Phys. Rev. E* **90** 022907
- [26] Kevrekidis P G, Theocharis G, Frantzeskakis D J and Malomed B A 2003 *Phys. Rev. Lett.* **90** 230401
- [27] Deng L, Hagley E W, Denschlag J, Simsarian J E, Edwards M, Clark C W, Helmerson K, Rolston S L and Phillips W D 1999 *Phys. Rev. Lett.* **83** 5407
- [28] Izrailev F M and Shepelyanskii D L 1980 *Theor. Math. Phys.* **43** 553
- [29] Bandrauk A D and Shen H 1994 *J. Phys. A: Math. Theor.* **27** 7147
- [30] Shrestha R K, Ni J, Lam W K, Wimberger S and Summy G S 2012 *Phys. Rev. A* **86** 043617
- [31] Sadgrove M and Wimberger S 2011 *Adv. At. Mol. Opt. Phys.* vol 60 (Amsterdam: Elsevier) ch 7, pp 315–69
- [32] Moore F L, Robinson J C, Bharucha C F, Sundaram B and Raizen M G 1995 *Phys. Rev. Lett.* **75** 4598  
Ringot J, Szriftgiser P, Garreau J C and Delande D 2000 *Phys. Rev. Lett.* **85** 2741  
d’Arcy M B, Godun R M, Oberthaler M K, Cassettari D and Summy G S 2001 *Phys. Rev. Lett.* **87** 074102  
Ryu C, Andersen M F, Vaziri A, Arcy M B, Grossman J M, Helmerson K and Phillips W D 2006 *Phys. Rev. Lett.* **96** 160403  
Behinaein G, Ramareddy V, Ahmadi P and Summy G S 2006 *Phys. Rev. Lett.* **97** 244101  
Kanem J F, Maneshi S, Partlow M, Spanner M and Steinberg A M 2007 *Phys. Rev. Lett.* **98** 083004  
Saijun W, Alexey T and Prentiss M G 2009 *Phys. Rev. Lett.* **103** 034101



- [33] Duffy G J, Parkins S, Müller T, Sadgrove M, Leonhardt R and Wilson A C 2004 *Phys. Rev. E* **70** 056206
- [34] Zhang C, Liu J, Raizen M G and Niu Q 2004 *Phys. Rev. Lett.* **92** 054101
- [35] Liu J, Wang W, Zhang C, Niu Q and Li B 2005 *Phys. Rev. A* **72** 063623
- Ullah A and Hoogerland M D 2011 *Phys. Rev. E* **83** 046218
- Martin J, Georgeot B and Shepelyansky D L 2008 *Phys. Rev. Lett.* **100** 044106
- [36] Shrestha R K, Wimberger S, Ni J, Lam W K and Summy G S 2013 *Phys. Rev. E* **87** 020902(R)